

Sub-harmonic Injection Locking in Metronomes

Tianshi Wang

Department of Electrical Engineering and Computer Sciences, University of California, Berkeley, CA, USA

Email: tianshi@berkeley.edu

Abstract

In this paper, we demonstrate sub-harmonic injection locking (SHIL) in mechanical metronomes. To do so, we first formulate metronome's physical compact model, focusing on its nonlinear terms for friction and the escapement mechanism. Then we analyze metronomes using phase-macromodel-based techniques and show that the phase of their oscillation is in fact very immune to periodic perturbation at twice its natural frequency, making SHIL difficult. Guided by the phase-macromodel-based analysis, we are able to modify the escapement mechanism of metronomes such that SHIL can happen more easily. Then we verify the occurrence of SHIL in experiments. To our knowledge, this is the first demonstration of SHIL in metronomes; As such, it provides many valuable insights into the modelling, simulation, analysis and design of nonlinear oscillators. The demonstration is also suitable to use for teaching the subject of injection locking and SHIL.

I. Introduction

Injection locking is an interesting phenomenon observed in almost all nonlinear oscillators. When an oscillator with natural frequency f_0 is perturbed by a small external periodic input at a frequency f_1 ($f_1 \approx f_0$), the oscillator will forget about its natural frequency and move its energy to lock to f_1 . Because of injection locking, coupled oscillators often synchronize in both frequency and phase. Many natural phenomena can be explained from this mechanism, such as the synchronization of fireflies' patterns, neurons firing in unison, *etc.* Injection locking is also widely used in the design of radio frequency communication circuits and optical lasers.

Perhaps the most famous example of injection locking in oscillators is the demonstration of metronomes synchronizing their ticks. As illustrated in Figure 1, when several metronomes are placed on a platform that can roll horizontally, each of them receives a small perturbation from their neighbours through the common platform. They may have slightly different central frequencies and may be started with random phases. But given some time, through the mechanism of injection locking, all of them will eventually lock to the same frequency with the same phase. This synchronization phenomenon is reproducible, easy to see and hear. As such, it is often used to illustrate or teach the subject of injection locking.

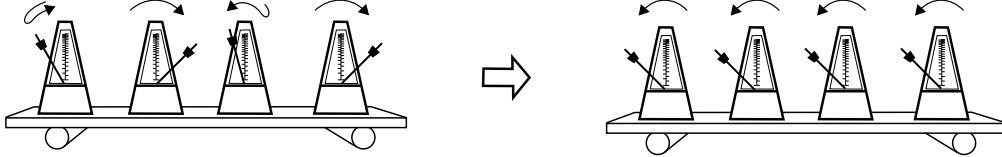


Fig. 1: Metronomes standing on a rolling board end up ticking in unison.

Sub-harmonic injection locking (SHIL) is a special type of injection locking. Under SHIL, oscillators are perturbed by a faster periodic input with a $2f_1$ frequency ($f_1 \approx f_0$). As illustrated in Figure 2, the oscillator will lock to f_1 , which is the sub-harmonic of the perturbation. SHIL has wide-ranging applications, such as in the design of high-performance quadrature oscillators [1], injection-locked PLLs [2], frequency dividers [3], optical lasers [4], *etc.* Recently, it has been shown that, through this mechanism, an oscillator can develop bistable phase responses that are suitable for encoding and storing phase-based logic bits for Boolean computation [5, 6]. This new computation paradigm has potential noise and power advantages over conventional level-encoded computation schemes. In this context, SHIL has been demonstrated in

CMOS ring oscillators and LC oscillators [5, 7].

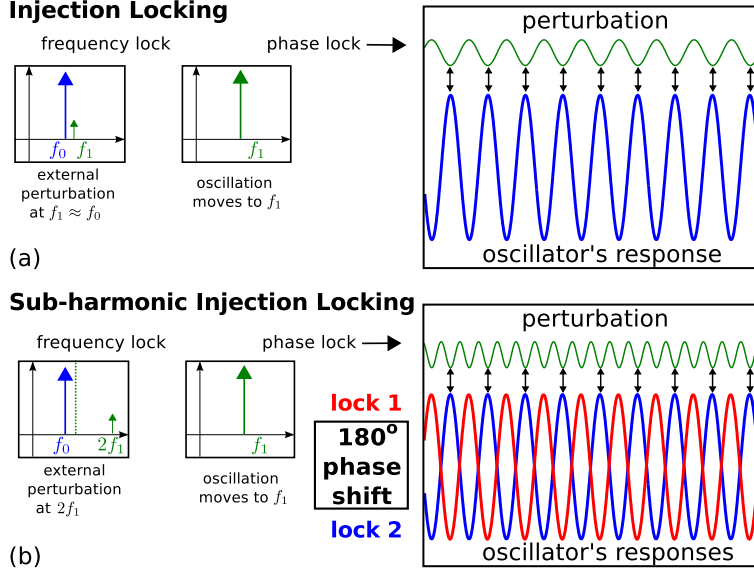


Fig. 2: Sub-harmonic Injection Locking implies phase lock with multiple stable phases. (a) When perturbing a self-sustaining oscillator (*e.g.*, a metronome) with input at f_1 close to its natural frequency f_0 , the oscillator moves its energy to f_1 and features phase lock. (b) When the perturbation is at $2f_1$, the oscillator may move to f_1 with bi-stable phase locking states.

However, SHIL has never been demonstrated in mechanical metronomes. The basic idea of such a demonstration is simple: just like in the scenario of regular injection locking (we refer to it as IL in the rest of the paper), two metronomes are placed on a rolling board — one oscillates at approximately the 1/2 sub-harmonic of the other. If SHIL happens, their swing patterns will synchronize. To complete this demonstration, they should also be decoupled by stopping the rolling board, in which case the synchronization ceases. Such a demonstration can show that SHIL is not limited to electrical oscillators — it is almost as universal as regular IL. It can also serve as an eye-catching illustration when teaching the subject of SHIL in classes.

The lack of such a demonstration is not because of lack of trying. In fact, we have been attempting to demonstrate it in our group for years. But simply tuning two metronomes to 1Hz and 2Hz¹ and putting them on a rolling board does not result in synchronization. The coupling seems to have little effect and the detuning in their frequencies remains, separating their phases apart. The metronomes we use² oscillate for approximately 17 min at 2Hz; clear and secure synchronization appears impossible to achieve within this time frame. This observation leaves us an impression that metronomes are very immune to perturbation close to its natural oscillation's second harmonic (we refer to it as second-order perturbation in the rest of this paper). This intuition needs more concrete analysis and justification.

In this paper, we adopt a more rigorous approach. We start with writing the physical model of metronomes in Sec. II. Then in Sec. III we use phase-macromodel-based techniques to analyze the model and debug why SHIL is hard to achieve. Then guided by the phase-macromodel analysis, we tweak the metronome, adjust its PPV such that SHIL can happen more easily. Finally, in Sec. IV, we validate the occurrence of SHIL in metronomes by experiments and measurements. As described above, we put a 1Hz metronome and a 2Hz metronome on a rolling board so that they can be coupled to each other; then we decouple them by putting them on a stationary board instead. In both scenarios, we tape colored labels to the rods of the metronomes, record videos and process them. Figure 3 shows the experimental setup and

¹Frequencies used in this paper are the frequencies of metronomes' oscillation. One cycle of metronome oscillation generates two ticks. So 1Hz and 2Hz metronomes generate 120 and 240 beats per minute respectively.

²Wittner Taktell Super-Mini Metronome

the key results. The curves in Figure 3 (b) and (d) are known as the Lissajous curves — they plot the x coordinates of the red dot *wrt* those of the blue dot. On a rolling board, Lissajous curves in Figure 3 (d) clearly show a pattern, indicating that the two metronomes synchronize. In the case of the stationary board, because of detuning, the Lissajous curves span the whole plane within the swings of oscillation.

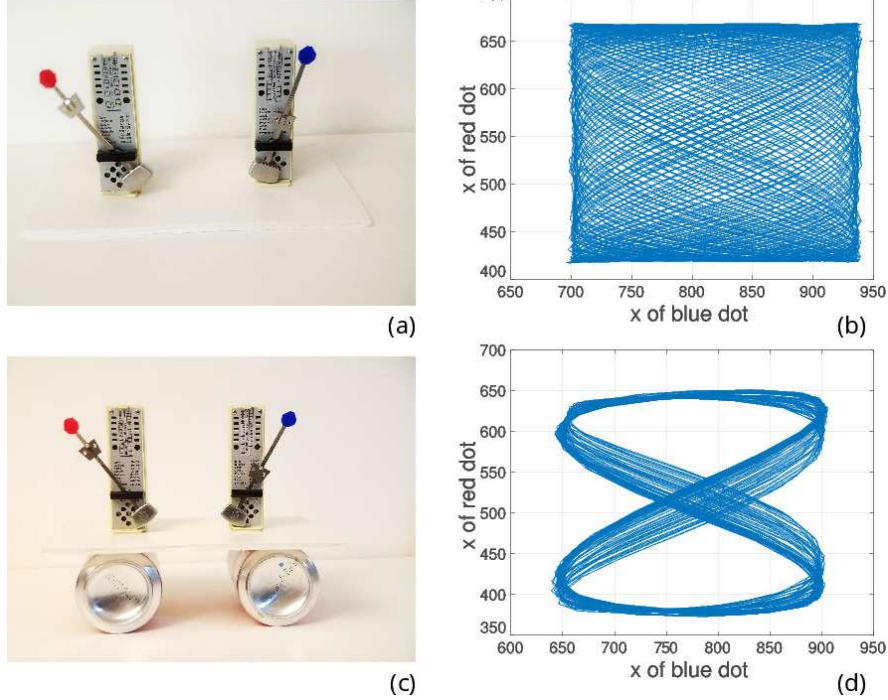


Fig. 3: (a) Two metronomes tuned to approximately 1Hz and 2Hz are placed on a stationary platform; (b) the corresponding Lissajou curves in show that no synchronization happens; (c) the metronomes are coupled through a rolling board; (d) the pattern in Lissajou curves demonstrates SHIL.

Along with the key results, this paper also presents compact models for metronomes that can run in open-source and commercial simulators, together with useful modelling techniques. Metronomes are normally modelled as lossless double-weighted pendulums [8, 9]. But the “lossiness” of an oscillator actually plays an important role in its injection locking behaviour. An accurate metronome model needs to include friction damping and also a mechanism known as escapement that compensates the energy lost every cycle due to friction. The implementations of the several existing metronome models with these mechanisms are not openly available. Neither are they formulated to be compatible with main-stream simulators. Moreover, friction and the escapement mechanism are often modelled in these models using non-smooth functions, making them not suitable for simulation. In our model, we use smooth functions to alleviate the difficulty of simulation convergence. As we explain in Sec. II, the use of smooth functions actually increases the models’ physical fidelity as well. The metronome models presented in this paper are implemented in both ModSpec/MATLAB and Verilog-A, and open-source released at [10]. In the Verilog-A version, we use the regular electrical discipline and model kinematic quantities as voltages, such that the model can be usable in as many simulators as possible.

To our knowledge, this is also the first time metronomes are analyzed using phase-macromodel-based techniques. Specifically, we extract a time-varying periodic vector — perturbation projection vector (PPV), from metronome model equations. PPV describes the sensitivity of the metronome’s phase to external perturbation. As we show in Sec. III, the fundamental frequency component and second harmonic of the PPV indicate how easy it is for IL and SHIL to happen. From the PPV numerical results, we confirm that SHIL is unlikely to occur without any modification to the metronome. And guided by the PPV results,

we can easily tweak the escapement mechanism such that SHIL can reliably happen.

The techniques we present in this paper on the modelling and analysis of metronomes, especially the use of phase-macromodels to predict, analyze and achieve desirable IL properties, are applicable and useful for the design of almost any oscillator. Moreover, the demonstration of SHIL shows that SHIL is a general phenomenon in nonlinear oscillators. Through this mechanism, a wide range of oscillators can potentially be used as phase-based binary latches — not just the electrical ones, but also those in optics, MEMS, bio-chemistry, spintronics, *etc.* Last but not least, the simulation and experimental results we present in this paper, are all easily reproducible. Just as metronomes are often used in teaching the subject of IL, the demonstration of SHIL in metronomes can also be used for teaching the subject of SHIL as well as oscillator modelling and design.

II. Modelling Metronomes

The dynamics of a metronome are mainly governed by the equation of a double-weighted pendulum. The equation is written using the angle θ and angular velocity $\dot{\theta} = \frac{d}{dt}\theta$ of the pendulum³:

$$\frac{d}{dt}\dot{\theta} = -\frac{1}{m_1 h_1^2 + m_2 h_2^2} \cdot (m_1 g \sin(\theta) \cdot h_1 - m_2 g \sin(\theta) \cdot h_2), \quad (1)$$

where m_1 is the mass of the weight at the bottom of the pendulum, h_1 is the distance from it to the axis of rotation; m_2 and h_2 are the mass and distance for the weight on the top of the pendulum; g is the gravitational constant.

Next, we add several terms to this pendulum equation — friction, the escapement mechanism, and external force.

Frictional forces in this system come from several sources: air friction, the axle bearing, and the contact between the tooth of the escapement wheel and the circular plate of the actuating member attached to the axle. The first one — air friction is often modelled as a viscous friction that grows linearly with velocity. The latter two are in the form of surface friction, which is often considered as a constant force in the opposite direction of the relative movement. They are much larger than the air friction in a metronome. Therefore, we write the formula for friction as

$$f(\dot{\theta}) = -f_0 \cdot \text{smoothsign}(\dot{\theta}), \quad (2)$$

where f_0 is a fitting parameter representing the constant amplitude of friction.

A double-weighted pendulum with only frictional forces will have damped oscillation. To sustain the oscillation, a metronome has a spring box inside that drives an escapement wheel through gears. The wheel has sloped teeth. At almost any time, one of the teeth is pushing against a circular plate attached to the axle of the pendulum. As the pendulum swings to certain angles where the circular plate is designed to have a gap, the wheel “escapes” through the plate and moves one tooth forward. In the meanwhile, the movement of the tooth pushes the circular plate, making the pendulum swing faster. At the same time, a sound of a tick is generated. This escapement happens twice during a cycle of oscillation, one when the pendulum is swing left and the other right. The angles at which the escapement occurs at left and right are normally symmetric. The pushing force on the pendulum generated by escapement is modelled as a $g(\theta, \dot{\theta})$ function in our model, which is non-zero only at small windows of θ , with direction aligned with the sign of $\dot{\theta}$.

$$\begin{aligned} g(\theta, \dot{\theta}) = & +g_0 \cdot (\text{smoothstep}(\theta - \theta_R) - \text{smoothstep}(\theta - \theta_R - \Delta\theta)) \cdot \text{smoothstep}(\dot{\theta}) \\ & -g_0 \cdot (\text{smoothstep}(\theta - \theta_L + \Delta\theta) - \text{smoothstep}(\theta - \theta_L)) \cdot \text{smoothstep}(-\dot{\theta}). \end{aligned} \quad (3)$$

The formula in (3) sets $g(\theta, \dot{\theta})$ to be about g_0 when $\theta_R < \theta < \theta_R + \Delta\theta$ and $\dot{\theta} > 0$; $g(\theta, \dot{\theta})$ is about

³The angle is defined between the pendulum and the vertical position. The direction does not change any equations.

$-g_0$ when $\theta_L - \Delta\theta < \theta < \theta_L$ and $\dot{\theta} < 0$.

Furthermore, the external force applied to a metronome can be written as a horizontal acceleration a of the axle of the pendulum.

Putting together all the components discussed above, we have a metronome model as follows.

$$\begin{aligned} \frac{d}{dt}\dot{\theta} = & -\frac{1}{m_1 h_1^2 + m_2 h_2^2} \cdot (m_1 g \sin(\theta) \cdot h_1 - m_2 g \sin(\theta) \cdot h_2 \\ & + f(\dot{\theta}) + g(\theta, \dot{\theta}) + m_1 \cdot a \cdot \cos(\theta) \cdot h_1 - m_2 \cdot a \cdot \cos(\theta) \cdot h_2). \end{aligned} \quad (4)$$

Among the parameters used in this model, m_1 , m_2 , h_1 and h_2 can be directly measured using a scale and a ruler; values for θ_R , θ_L and $\Delta\theta$ can be obtained by measuring the gap in the circular plate using a protractor. f_0 is the nominal value of friction. We can estimate it by letting the pendulum swing within small angles, such that the escapement does not happen. In this case, the metronome begins damped oscillation due to friction. We can tweak the value of parameter f_0 until the simulated response matches observation in the speed of damping. g_0 is the force the escapement wheel applies to the pendulum during each tick. When all the other parameters are fixed, g_0 determines the swing of the metronome. We can estimate this parameter by matching the magnitude of oscillation in simulation with the actual swing of the metronome. From above, we have been able to systematically determine all the parameters in the metronome model (4), either directly or indirectly.

Note that in the model equations for friction (2) and escapement mechanism (3), we use the smooth versions of sign and step functions [11]. This is not just for improving the convergence of numerical simulation. The use of smooth functions also makes the model represent the physical system more truthfully. For example, when the tooth of the escapement wheel starts to push the circular plate, the force is not instantaneous because the surface at the edge of the gap is still smooth. Similarly, representing friction using smooth functions also increases the model's physical fidelity [12].

A. Metronome Model in MAPP

To run simulation algorithms on this metronome model, we implement it in MAPP, the Berkeley Model and Algorithm Prototyping Platform. MAPP models general continuous-time dynamical systems as differential algebraic equations (DAEs). A DAE has the following format:

$$\frac{d}{dt}\vec{q}(\vec{x}(t), \vec{u}(t)) + \vec{f}(\vec{x}(t), \vec{u}(t)) = \vec{0}. \quad (5)$$

In the metronome model, $\vec{x} = [\theta, \dot{\theta}]^T$, $\vec{u} = [a]$. By specifying functions \vec{q} and \vec{f} , we can write this model in the DAE format.

$$\vec{q}(\vec{x}(t), \vec{u}(t)) = - \begin{bmatrix} \theta \\ \dot{\theta} \end{bmatrix} = -\vec{x} \quad (6)$$

$$\vec{f}(\vec{x}(t), \vec{u}(t)) = \begin{bmatrix} \dot{\theta} \\ \frac{d}{dt}\dot{\theta} \text{ in equation (4)} \end{bmatrix} \quad (7)$$

MAPP provides a convenient way of coding this model in the MATLAB[®] language. The code is shown in Appendix A-A.

Results from transient analysis in Figure 4 show that the model reproduces the self-sustaining oscillation observed in metronomes. Note that the waveforms of θ and $\dot{\theta}$ are not perfectly sinusoidal, $\dot{\theta}$ actually has two small notches every cycle — they are where the escapement wheel moves forward one tooth. Plot of $g(\theta, \dot{\theta})$ function in Figure 5 demonstrates this mechanism more clearly; unlike a spring-mass system or a single pendulum, a metronome is indeed a nonlinear oscillator with highly non-smooth dynamics.

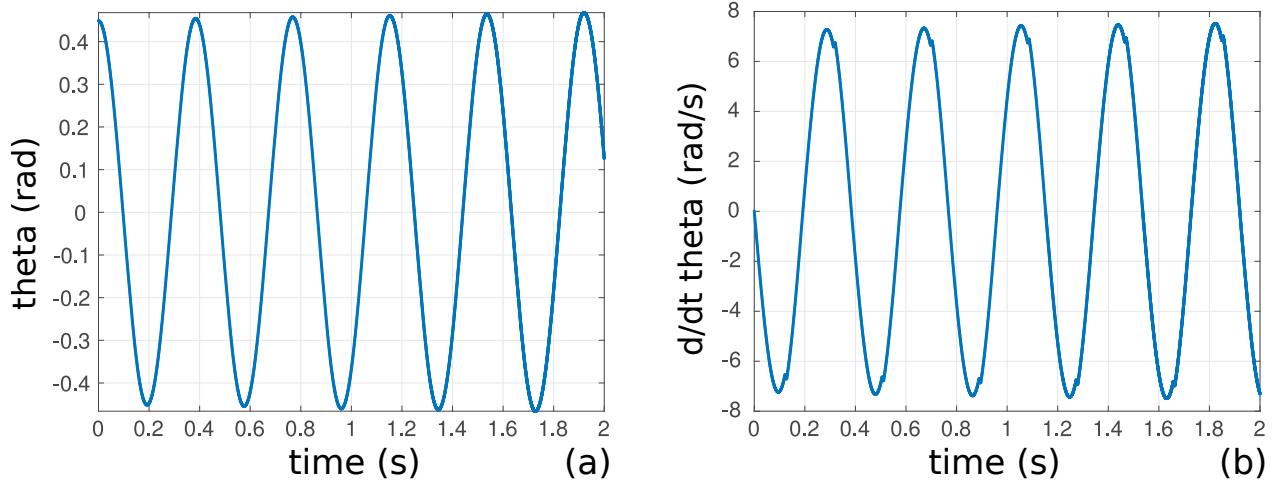


Fig. 4: Transient simulation results of θ and $\dot{\theta}$ from MAPP.

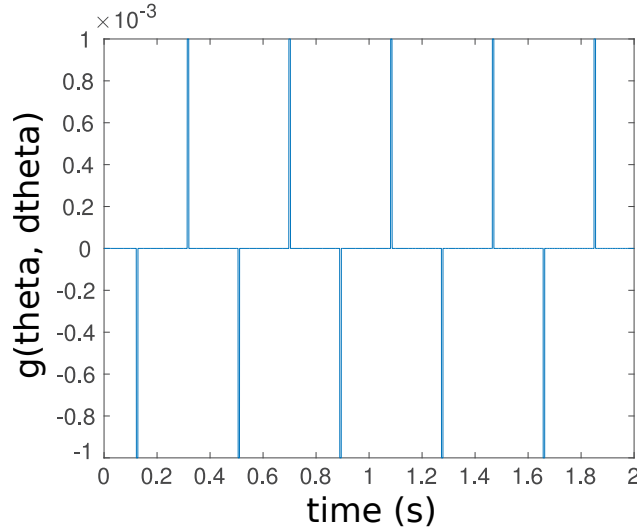


Fig. 5: Transient simulation results of $g(\theta, \dot{\theta})$ from MAPP.

B. Metronome Model in Verilog-A

We can also implement the metronome model in the Verilog-A language and simulate it in commercial circuit simulators. Verilog-A is an industry-standard modelling language designed mainly for electronic devices. For the metronome model to run in most simulators, we do not use Verilog-A's multiphysics disciplines; we use only electrical domain constructs. θ and $\dot{\theta}$ can be modelled as two voltages.⁴ The Verilog-A code for the metronome model is shown in Appendix A-B. It generates consistent results as in Figure 4 and Figure 5 in commercial simulator Spectre®.

III. Phase-macromodels of Metronomes

In Figure 4, one can see that the waveforms' amplitudes increase slightly with time; the oscillation has not settled to the limit cycle yet. Instead of waiting for it to settle in transient simulation, we can use other algorithms to directly capture the limit cycle, *aka*, the Periodic Steady State (PSS). There are two common PSS algorithms — the shooting method, which is based on transient analysis, and harmonic balance, which

⁴ $\dot{\theta}$ can be a current charging the θ node. But for printing and plotting, it is more convenient to define it as a voltage.

is a mixed frequency/time domain method. Both are implemented in MAPP and in Spectre[®]. PSS analysis computes an oscillator's response $\vec{x}_s(t)$ such that

$$\vec{x}_s(t) = \vec{x}_s(t + T_0), \quad (8)$$

where $T_0 = 1/f_0$ is the period of oscillation.

When the oscillator is under a small perturbation $\vec{u}(t)$, its oscillation along the limit cycle develops a phase deviation $\alpha(t)$. The oscillator's response under perturbation can be written as

$$\vec{x}(t) = \vec{x}_s(t + \alpha(t)), \quad (9)$$

where $\alpha(t)$ is governed by a differential equation:

$$\frac{d}{dt}\alpha(t) = \vec{v}^T(t + \alpha(t)) \cdot \vec{u}(t). \quad (10)$$

Equation (10) is the phase macromodel of the oscillator; it can directly capture the phase response under perturbation. The time-varying periodic vector \vec{v} inside equation (10) is known as the perturbation projection vector (PPV). It can be numerically calculated from both shooting and harmonic balance.

When the external perturbation $\vec{u}(t)$ is periodic itself with frequency $f_1 = 1/T_1$, equation (10) can be rewritten as

$$\frac{d}{dt}\Delta\phi(t) = f_0 - f_1 + f_0 \cdot \vec{v}_{(1)}^T(f_1 \cdot t + \Delta\phi(t)) \cdot \vec{u}_{(1)}(f_1 \cdot t), \quad (11)$$

where $\Delta\phi(t) = (f_0 - f_1) \cdot t + f_0 \cdot \alpha(t)$ — when injection locking occurs, it is the phase difference between the oscillator's response and the periodic perturbation; $\vec{v}_{(1)}$ and $\vec{u}_{(1)}$ are 1-periodic functions — $\vec{v}_{(1)}(t) = \vec{v}(T_0 \cdot t)$, $\vec{u}_{(1)}(t) = \vec{u}(T_1 \cdot t)$.

Then we expand 1-periodic functions $\vec{v}_{(1)}$ and $\vec{u}_{(1)}$ with their Fourier coefficients $\{\vec{v}_{k(1)}\}$ and $\{\vec{u}_{l(1)}\}$:

$$\vec{v}_{(1)}(f_1 t + \Delta\phi(t)) = \sum_{k=-\infty}^{k=\infty} \vec{v}_{k(1)} \cdot e^{j2\pi(kf_1 t + k\Delta\phi(t))}, \quad (12)$$

$$\vec{u}_{(1)}(f_1 t) = \sum_{l=-\infty}^{l=\infty} \vec{u}_{l(1)} \cdot e^{j2\pi(lf_1 t)}. \quad (13)$$

Therefore, (11) can be written as a double summation in the Fourier domain:

$$\frac{d}{dt}\Delta\phi(t) = f_0 - f_1 + f_0 \sum_{k=-\infty}^{k=\infty} \sum_{l=-\infty}^{l=\infty} \vec{v}_{k(1)}^T \cdot \vec{u}_{l(1)} \cdot e^{j2\pi(kf_1 \cdot t + k\Delta\phi(t) + lf_1 t)}. \quad (14)$$

Simplification of (14) results in the Generalized Adler's Equation (GAE) [13], and it provides good approximations to the injection-locked solutions of (11).

When $\vec{u}(t)$ contains only the second-order perturbation, *i.e.*, it is sinusoidal with a frequency of $2f_1$, $\vec{u}_{2(1)} = \vec{u}_{-2(1)}^* \neq 0$ are the only non-zero coefficients in $\{\vec{u}_{l(1)}\}$. From the analyses in [14], the larger the magnitude of $\vec{v}_{2(1)}$, the more detuning between f_1 and f_0 the oscillator can endure while still having an injection-locked solution.

Figure 6 and Figure 7 show the time- and frequency-domain PPV of a metronome. The metronome model has only one input variable a , which is the horizontal external input acceleration; the PPV becomes a time-varying scaler that describes the phase's sensitivity to this input. From Figure 7 we see that the PPV has a large coefficient at the fundamental frequency, indicating that a metronome is prone to regular first-order IL. But the second harmonic of the PPV is around 10^{-12} , in the order of numerical noise. In fact, all even harmonics are practically zero, because both the waveforms and PPV of a metronome are designed to be odd symmetric. It would be easier to SHIL the metronome with a periodic input $u(t)$ at $3f_1$, but if we insist on using $2f_1$, the metronome needs to be modified.

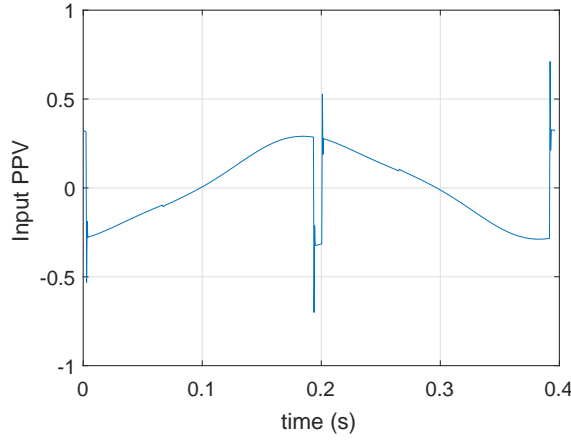


Fig. 6: Input PPV of metronome.

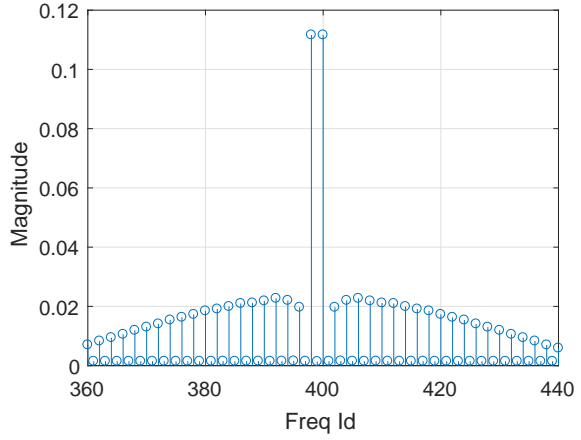


Fig. 7: Frequency domain coefficients of metronome's PPV.

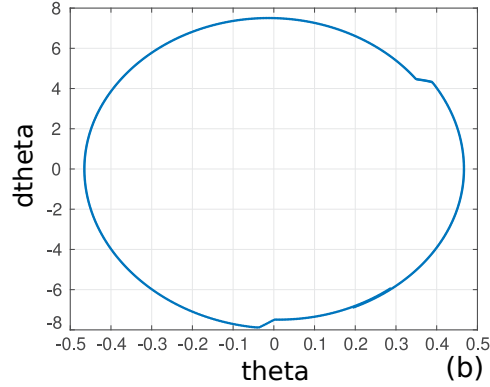
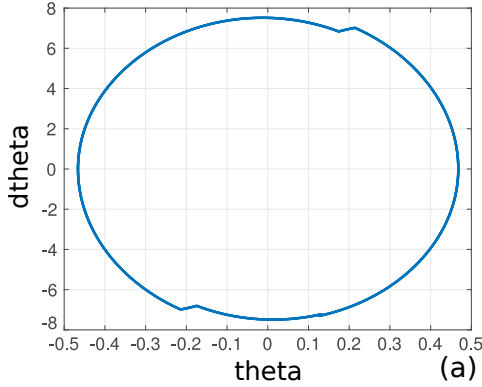


Fig. 8: Phase portrait of a metronome's oscillation before and after modification.

The phase portrait in Figure 8 (a) illustrates the oscillation of a metronome; it is another way of visualizing the θ and $\dot{\theta}$ waveforms in Figure 4. The two small kinks in the loop result from the escapement mechanism, which accelerates $\dot{\theta}$ for a short time. They are symmetric about the origin. If we open up the metronome, use pliers to rotate the circular plate, we can adjust the values of θ_R and θ_L in (3), thus making the phase portrait asymmetric, as illustrated in Figure 8 (b). After this modification, the two ticks generated in each cycle are not equally separated anymore. But interestingly, the duration of the metronome oscillation does not change; the modification does not seem to affect the metronome's energy consumption.

Figure 9 and Figure 10 show the PPV of the metronome after modification. Compared against Figure 6 and Figure 7, the second harmonic of the PPV increases from zero to 0.028, which is now about 43% of the coefficient at fundamental frequency. The observation of SHIL should now becomes considerably easier; it should be almost as reproducible as regular IL in metronomes.

IV. Experimental Results

As described in Sec. I, we placed two metronomes on a rolling board — one tuned to around 1Hz, the other around 2Hz. The 1Hz metronome was modified according to Sec. III. A red sticker was taped to the rod of the 1Hz metronome; a blue one to the 2Hz metronome. With a tripod, we recorded their oscillation with a 30Hz frame rate. The video was imported frame by frame into MATLAB[®]; an simple algorithm was used to extract the locations of red and blue stickers from the video. For every frame, we determined the centers of the two stickers by selecting fixed numbers of red-most and blue-most pixels and averaging their locations respectively. Figure 11 (d) shows the oscillation in the two stickers' x coordinates within

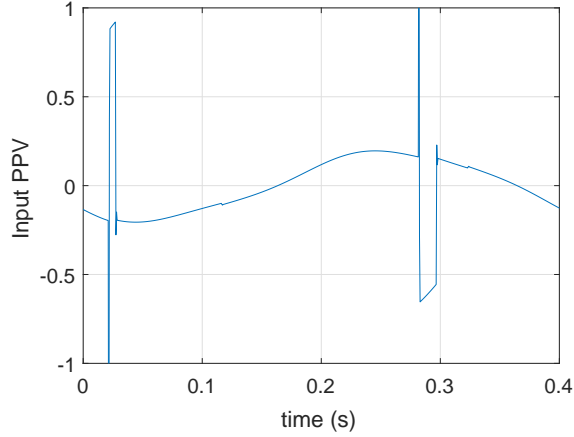


Fig. 9: Input PPV of modified metronome.

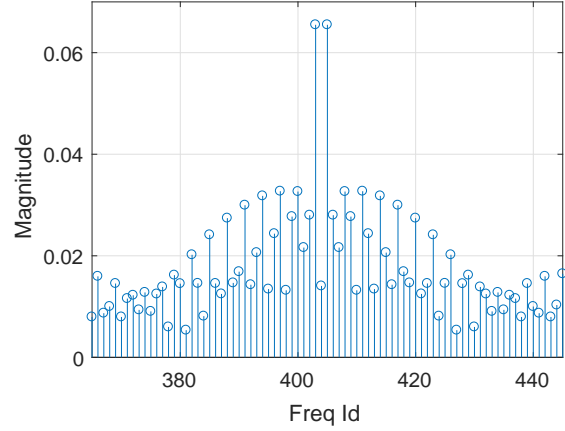
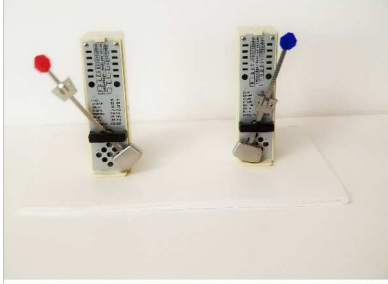
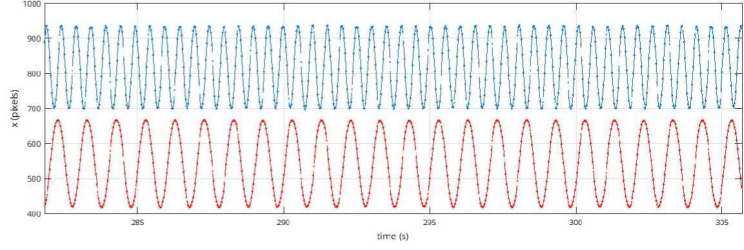


Fig. 10: Frequency domain coefficients of modified metronome's PPV.

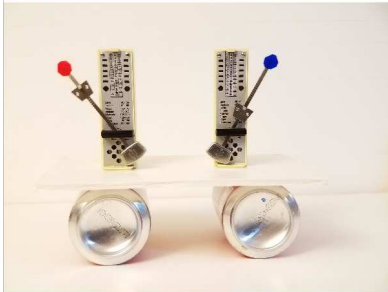
a time frame of about 20 seconds.



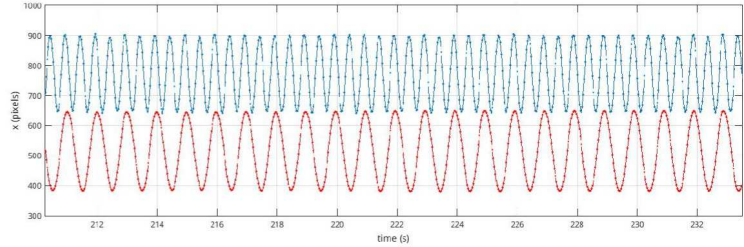
(a)



(b)



(c)



(d)

Fig. 11: (a) Two metronomes placed on a stationary board; (b) corresponding waveforms of the tips of their pendulum rods; (c) two metronomes on a rolling board; (d) their corresponding waveforms.

Similarly, without retuning the metronomes, we placed them on a stationary board instead, processed the video and plotted the oscillation in Figure 11 (b). Throughout the plot, the peaks of the red waveform are almost aligned to every other valleys of the blue waveform. However, at the beginning of the plot, the red peak is on the right of the blue valley, but towards the end of the plot, it has clearly drifted to the left of the corresponding blue valley. This is an indication that the two metronomes are not synchronized, whereas in Figure 11 (d), the two waveforms are aligned within the same duration, indicating the occurrence of SHIL.

We can also identify all the peaks in Figure 11 (b) and (d) with the help of a MATLAB[®] command `findpeaks()`. Based on the locations of the peaks, we can plot the phase difference between the two metronomes in Figure 12. When the two metronomes are free running on a stationary board, the phase

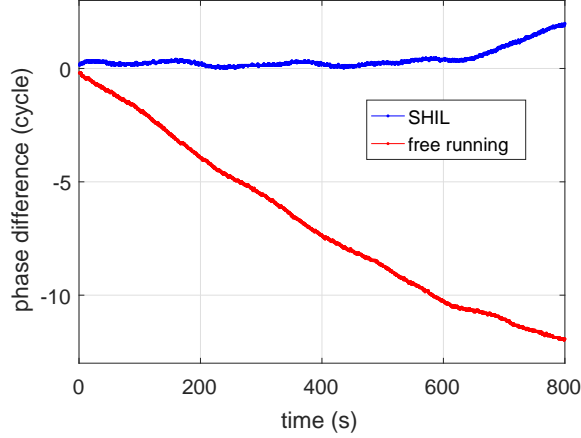


Fig. 12: Phase difference between the 2Hz and 1Hz metronomes. The difference is measured by the number of cycles of the 1Hz metronome. Positive values mean that the 1Hz metronome is leading the 2Hz one.

difference keeps increasing. Specifically, the 1Hz metronome lags the 2Hz one by approximately 10 cycles after 600 seconds. But when they are on the rolling board, the phase difference stays constant around zero for the same duration. Put in other words, every 2 cycles of the 2Hz metronome align almost perfectly with 1 cycle of the 1Hz one. The measurements are not perfectly flat mainly because the spring box does not generate a constant force, and a metronome's frequency changes slightly as the spring unrolls. Also, as the two metronomes oscillate beyond 10 minutes towards the end of their oscillation, their frequencies drift more and more, and SHIL is eventually broken.

Furthermore, from the locations of the peaks, we can calculate the frequencies of the two metronomes. From the stationary board to the rolling board, the 2Hz metronome maintains the same frequency at $2f_1 = 1.978$, but the 1Hz one changes its frequency by about 1%, from $f_0 = 0.998$ to $f_1 = 0.989$. This indicates that it is the slower metronome that moves its frequency from f_0 to f_1 , same as our expectation in Sec. I.

V. Summary

This paper demonstrates SHIL in mechanical metronomes. Along the way, we introduce and open-source release compact models for metronomes that are accurate, physical and can work well in almost all open-source and commercial simulators. We also analyze metronomes with PPV-based techniques, which in return guide us in designing a modification to metronomes to make them more suitable for SHIL. The phase-locked states from SHIL enable an oscillator to store phase-based logic values and make almost all oscillators potential candidates for Boolean computation. Demonstrating bit storage in a metronome requires another metronome injection locked to the same frequency to provide a phase reference. For example, in the setup in this paper, another 1Hz metronomes also locked to the 2Hz one is needed to distinguish between the two locked states. This will be part of our future work.

References

- [1] P. Kinget, R. Melville, D. Long, and V. Gopinathan. An injection-locking scheme for precision quadrature generation. *Solid-State Circuits, IEEE Journal of*, 37(7):845–851, 2002.
- [2] D. Abramovitch. Phase-locked loops: a control centric tutorial. In *Proc. American Control Conference*, volume 1, pages 1 – 15 vol.1, May 2002.
- [3] M. Tiebout. A CMOS direct injection-locked oscillator topology as high-frequency low-power frequency divider. *Solid-State Circuits, IEEE Journal of*, 39(7):1170–1174, 2004.
- [4] L. Goldberg, H.F. Taylor, J.F. Weller, and D.M. Bloom. Microwave signal generation with injection-locked laser diodes. *Electronics Letters*, 19(13):491–493, June 1983.
- [5] T. Wang and J. Roychowdhury. PHLOGON: PHase-based LOGic using Oscillatory Nanosystems. In *Proc. UCNC*, LNCS sublibrary: Theoretical computer science and general issues. Springer, July 2014. DOI link.
- [6] J. Roychowdhury. Boolean Computation Using Self-Sustaining Nonlinear Oscillators. *arXiv:1410.5016v1 [cs.ET]*, Oct 2014.

arXiv:1410.5016v1.

- [7] T. Wang and J. Roychowdhury. Design Tools for Oscillator-based Computing Systems. In *Proc. IEEE DAC*, pages 188:1–188:6, 2015. DOI link.
- [8] J. Pantaleone. Synchronization of Metronomes. *American Journal of Physics*, 70(10):992–1000, 2002.
- [9] J. Jia, Z. Song, W. Liu, J. Kurths, J. Xiao. Experimental Study of the Triplet Synchronization of Coupled Nonidentical Mechanical Metronomes. *Scientific reports*, 5, 2015.
- [10] Metronome Model Release. Web site: <https://github.com/TianshiWang/metronome>.
- [11] T. Wang and J. Roychowdhury. Well-Posed Models of Memristive Devices. *arXiv preprint arXiv:1605.04897*, 2016.
- [12] C. Makkar, W.E. Dixon, W.G. Sawyer, and G. Hu. A new continuously differentiable friction model for control systems design. In *Advanced Intelligent Mechatronics. Proceedings, 2005 IEEE/ASME International Conference on*, pages 600–605. IEEE, 2005.
- [13] P. Bhansali and J. Roychowdhury. Gen-Adler: The generalized Adler’s equation for injection locking analysis in oscillators. In *Proc. IEEE ASP-DAC*, pages 522–227, January 2009. DOI link.
- [14] A. Neogy and J. Roychowdhury. Analysis and Design of Sub-harmonically Injection Locked Oscillators. In *Proc. IEEE DATE*, Mar 2012. DOI link.

Appendix A

Model Code for a Single Metronome

A. metronomeDAE.m: model file for metronome DAE in MAPP

```
1 function DAE = single_metronome_w_input()
2     DAE = init_DAE();
3
4     DAE = add_to_DAE(DAE, 'name', 'single metronome');
5     DAE = add_to_DAE(DAE, 'unkname(s)', {'theta', 'thetadot'});
6     DAE = add_to_DAE(DAE, 'eqnname(s)', {'thetadot', 'thetadotdot'});
7     DAE = add_to_DAE(DAE, 'inputname(s)', {'a'}); % acceleration
8     DAE = add_to_DAE(DAE, 'outputname(s)', {'theta'});
9     DAE = add_to_DAE(DAE, 'parm(s)', {'m1', 0.1, ...
10                                     'm2', 0.01, ...
11                                     'h1', 2e-2, ...
12                                     'h2', 4e-2, ...
13                                     'f0', 2e-4, ...
14                                     'g0', 5e-3, ...
15                                     'thetaL', -pi/18, ...
16                                     'thetaR', pi/18, ...
17                                     'dtheta', pi/80, ...
18                                     'g', 9.81, ...
19                                     'smoothing', 1e-10});
20
21     DAE = add_to_DAE(DAE, 'B', @B);
22     DAE = add_to_DAE(DAE, 'C', @C);
23     DAE = add_to_DAE(DAE, 'D', @D);
24
25     DAE = add_to_DAE(DAE, 'f_takes_inputs', 1);
26     DAE = add_to_DAE(DAE, 'f', @f);
27     DAE = add_to_DAE(DAE, 'q', @q);
28
29     DAE = finish_DAE(DAE);
30 end
31
32 function out = B(S)
33     out = [];
34 end
35
36 function out = C(DAE)
37     out = [1 0];
38 end
39
40 function out = D(DAE)
41     out = [];
42 end
43
44 function fout = f(S)
45     v2struct(S);
46     thetadotdot = - 1 / (m1*h1^2 + m2*h2^2) * (...
47         + m1*g*sin(theta)*h1 - m2*g*sin(theta)*h2 ...
48         - friction(thetadot, f0, smoothing) ...
49         - gfunc(theta, thetadot, g0, thetaL, thetaR, dtheta, smoothing) ...
50         + m1*a*cos(theta)*h1 - m2*a*cos(theta)*h2);
```

```

50     thetadotdef = thetadot;
51     fout = [thetadotdef; thetadotdot];
52 end % f(...)
53
54 function gout = q(S)
55     gout = [-S.theta; -S.thetadot];
56 end % q(...)
57
58 function out = friction(thetadot, f0, smoothing)
59     out = - f0 * smoothsign(thetadot, smoothing);
60 end
61
62 function out = gfunc(theta, thetadot, g0, thetaL, thetaR, dtheta, smoothing)
63     out = g0 * (smoothstep(theta-thetaR, smoothing) ...
64         - smoothstep(theta-thetaR-dtheta, smoothing)) ...
65         .* smoothstep(thetadot, smoothing) ...
66         - g0 * (smoothstep(theta-thetaL+dtheta, smoothing) ...
67         - smoothstep(theta-thetaL, smoothing)) .* smoothstep(-thetadot, smoothing);
68 end

```

Listing 1: metronomeDAE.m

B. metronome.va: Verilog-A model for a single metronome with acceleration input.

```

1  `include "disciplines.vams"
2  `include "constants.vams"
3
4  module single_metronome_w_input(ntheta, ntheta_dot, na, gnd);
5      inout ntheta, ntheta_dot, na, gnd;
6      electrical ntheta, ntheta_dot, na, ng, gnd;
7
8      parameter real m1 = 0.1 from (0:inf);
9      parameter real m2 = 0.01 from (0:inf);
10     parameter real h1 = 2e-2 from (0:inf);
11     parameter real h2 = 4e-2 from (0:inf);
12     parameter real f0 = 5e-4 from [0:inf];
13     parameter real g0 = 1e-2 from [0:inf];
14     parameter real thetaL = -`M_PI/10 from (-inf:inf);
15     parameter real thetaR = `M_PI/10 from (-inf:inf);
16     parameter real dtheta = `M_PI/40 from (0:inf);
17     parameter real g = 9.81 from (0:inf);
18     parameter real smoothing = 1e-10 from [0:inf];
19     parameter real current_scaling = 1e-6 from [0:inf];
20
21     real theta, thetadot, a;
22
23     `include "smoothfunctions.vams"
24
25     analog function real friction;
26         input thetadot, f0, smoothing;
27         real thetadot, f0, smoothing;
28         begin
29             friction = - f0 * smoothsign(thetadot, smoothing);
30         end
31     endfunction // friction
32
33     analog function real gfunc;
34         input theta, thetadot, g0, thetaL, thetaR, dtheta, smoothing;
35         real theta, thetadot, g0, thetaL, thetaR, dtheta, smoothing;
36         begin
37             gfunc = g0 * (smoothstep(theta-thetaR, smoothing)
38                 - smoothstep(theta-thetaR-dtheta, smoothing)) *
39                 smoothstep(thetadot, smoothing)
40                 - g0 * (smoothstep(theta-thetaL+dtheta, smoothing)
41                 - smoothstep(theta-thetaL, smoothing)) *
42                 smoothstep(-thetadot, smoothing);
43         end
44     endfunction // gfunc

```

```

45
46 analog begin
47     theta = V(ntheta, gnd);
48     thetadot = V(nthetadot, gnd);
49     a = V(na, gnd);
50
51     I(ntheta, gnd) <+ current_scaling * thetadot;
52     I(ntheta, gnd) <+ ddt(- current_scaling * theta);
53
54     I(nthetadot, gnd) <+ - 1 / (m1*pow(h1,2) + m2*pow(h2,2)) * current_scaling *
55         ( + m1*g*sin(theta)*h1 - m2*g*sin(theta)*h2
56           - friction(thetadot, f0, smoothing)
57           - gfunc(theta, thetadot, g0, thetaL, thetaR, dtheta, smoothing)
58           + m1*a*cos(theta)*h1 - m2*a*cos(theta)*h2);
59     I(nthetadot, gnd) <+ ddt(- current_scaling * thetadot);
60
61     I(na, gnd) <+ 0;
62 end
63 endmodule

```

Listing 2: metronome.va